

Double-modulation CPT cesium compact clock

Peter Yun¹, Sinda Mejri¹, Francois Tricot¹, Moustafa Abdel Hafiz²,
Rodolphe Boudot², Emeric de Clercq¹, Stéphane Guérandel¹

¹ LNE-SYRTE, Observatoire de Paris, PSL Research University, CNRS, Sorbonne Universités, UPMC Univ. Paris 06, 61 avenue de l'Observatoire, 75014 Paris, France

² FEMTO-ST, CNRS, UFC, 26 chemin de l'épitaphe 25030 Besançon cedex, France

E-mail: enxue.yun@obspm.fr

Abstract. Double-modulation coherent population trapping (CPT) is based on a synchronous modulation of Raman phase and laser polarization, which allows the atomic population to accumulate in a common dark state. The high contrast signal obtained on the clock transition with a relative compact and robust laser system is interesting as basis of a high performance microwave clock. Here we study the parameters of a double-modulation CPT Cs clock working in cw mode. The optimal polarization modulation frequency and cell temperature for maximum contrast of clock transition are investigated. The parameters of the detection are also studied. With the optimal parameters, we observe a CPT signal with contrast of 10% and linewidth of 492 Hz, which is well suited for implementing a cw atomic clock.

1. Introduction

Vapor cell frequency standards [1, 2] are of prime interest in all applications where frequency stability and size are the major criterion, such as satellite on-board clocks. This field has known outstanding progress since a few years with laboratory clocks exhibiting frequency stabilities at 1 s in the $1 - 3 \times 10^{-13}$ range, i.e. a gain of almost two order of magnitudes on present Rb clocks. These new clocks are based on the double-resonance technique [3], pulsed optical pumping and microwave interrogation [4, 5], or coherent population trapping (CPT) [6, 7]. CPT clocks need a circularly polarized laser beam to create a state superposition, the dark state, in the ground state of alkali-metal atoms [8, 9]. High performance CPT clocks need more sophisticated schemes in order to increase the contrast by avoiding the optical pumping and the trapping of the atoms into the end Zeeman sublevels. The lin \perp lin method [10, 11] needs two phase-locked lasers to provide two linearly and orthogonally polarized laser beams. The push-pull optical pumping (PPOP) [12, 13] reduces this complexity by using a single laser plus a Michelson type set-up, which introduces a phase shift between two counter-rotating circularly polarized beams. Without this phase shift the dark state built by a polarization is destroyed by the other one. In our double-modulation scheme [14], both the Raman phase and laser polarization are synchronously modulated to realize a time-version of push-pull optical pumping. Contrary to the PPOP configuration which separates and recombines the laser beams, our scheme provides a simple and robust laser bench by utilizing a polarization switch.

In our scheme, the polarization of a bichromatic laser beam is modulated between two opposite circular polarizations [15]. An appropriate modulation of the phase between the two components of the bichromatic laser beam, the so-called Raman phase, is applied



synchronously. The two CPT dark states, produced successively by the alternate polarizations, add constructively. Owing to this additional Raman phase modulation, the common dark state is decoupled from the laser at all times. For these two reasons, i.e., the atomic population accumulated into the clock states and the constructive build-up of two CPT dark states, a high contrast signal of the clock transition is observed. Another advantage of this scheme is the absence of $\Delta m_F = 2$ spurious CPT transitions [16, 17], here m_F is the magnetic quantum number. Moreover, our scheme provides compact and robust system for CPT atomic clock, in which only one-laser system is utilized, the polarization switch should be less vibration sensitive than a Michelson type set-up. Here we study the detail of double-modulation CPT clock work in cw mode. Experimental parameters, e.g., cell temperature, modulation frequency, detected window duration and delay are investigated. The short term frequency stability based on the measured relative intensity noise of our laser beam is estimated.

2. Experimental set-up

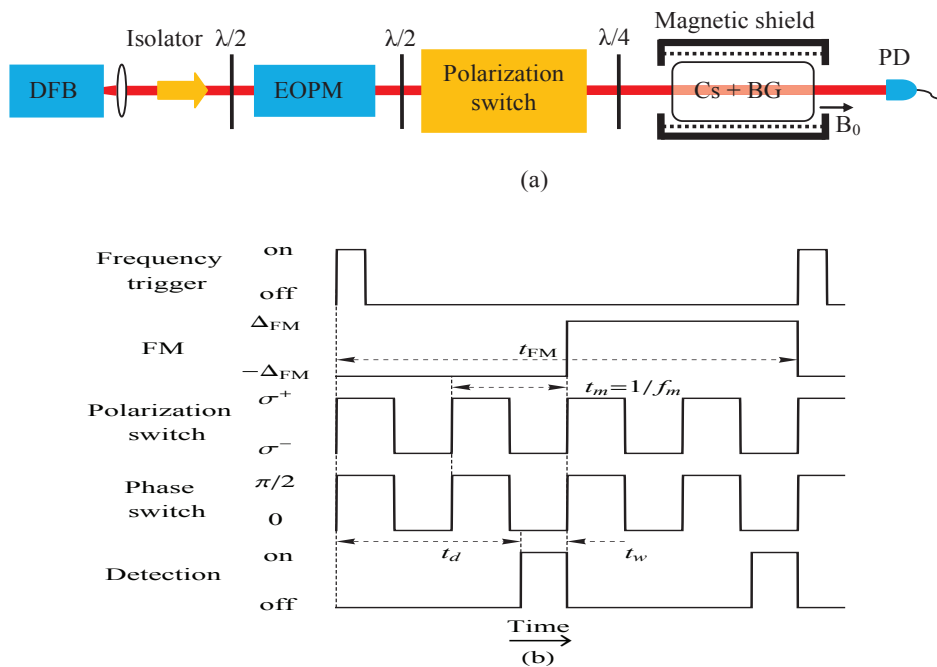


Figure 1: (a)(Color online) Double-modulation CPT setup. (b) Pulse sequence. The abbreviation, DFB: distributed feedback diode laser, EOPM: electro-optic phase modulator, BG: buffer gas, PD: photodiode. FM: frequency modulation.

As shown in figure 1(a), a distributed feedback diode (DFB) emits a monochromatic laser beam tuned on the D_1 line of Cesium. After passing through a fiber electro-optic phase modulator (EOPM), driven at 4.6 GHz with 26 dBm microwave power, a bichromatic laser is formed by the ± 1 first sidebands of the modulated spectrum. The $-1(+1)$ st sideband is tuned to the transitions $|6^2S_{1/2}, F = 4(3)\rangle \leftrightarrow |6^2P_{1/2}, F' = 4\rangle$. A $0 - \pi/2$ phase modulation is added to the 4.6 GHz microwave, thus the optical Raman phase is modulated between 0 and π . Joint with a polarization modulator, synchronously modulated with the Raman phase, we get a double-modulated Raman laser. The polarization modulator is formed by an amplitude electro-optic modulator (EOM, Thorlabs: EO-AM-NR-C2), which shows 18 dB extinction ratio of polarization and 2.5 μ s rising and falling time. A quarter-wave plate converts the perpendicular

linear polarizations in opposite circular polarizations. The double-modulated Raman laser beam is then expanded to a diameter of 10 mm before the glass cell. The cylindrical Cs vapor cell, 20 mm diameter and 50 mm long, is filled with 21 Torr of mixed buffer gas (argon and nitrogen). Unless otherwise specified, the cell temperature is stabilized at 37.5 °C. A solenoid coil surrounded by two magnetic shields provides a uniform magnetic field of 4.82 μ T in order to remove the Zeeman degeneracy.

The pulse sequence displayed in figure 1(b) is designed for cw double-modulation CPT, in which the $0 - \pi/2$ microwave phase and the $\sigma^- - \sigma^+$ polarization are synchronously modulated at frequency f_m to prepare constructive CPT states. The signal is recorded by a photodiode with a time delay t_d after the beginning of the sequence and during a time t_w .

To obtain a discriminator signal, the usually employed frequency modulation (FM) technique is adopted, i.e., in the two successive half periods of FM, the microwave frequency is up and down shifted Δ_{FM} relative to the un-modulated one f_0 respectively, the correspondent photo-detector (PD) signals are subtracted, an error signal is then obtained after a low pass filter when we scan the microwave frequency f_0 .

3. Results

3.1. CPT spectrum and contrast

A typical Zeeman CPT spectrum is demonstrated in figure 2(a). The seven peaks observed are the seven allowed transitions between the hyperfine ground states of same magnetic quantum number m_F , $m_F = -3$ to $+3$. The central and highest peak is the clock transition ($0 - 0$). This clearly shows that the atomic population is effectively collected in the clock states. The distortion of side peaks is explained by magnetic field inhomogeneity.

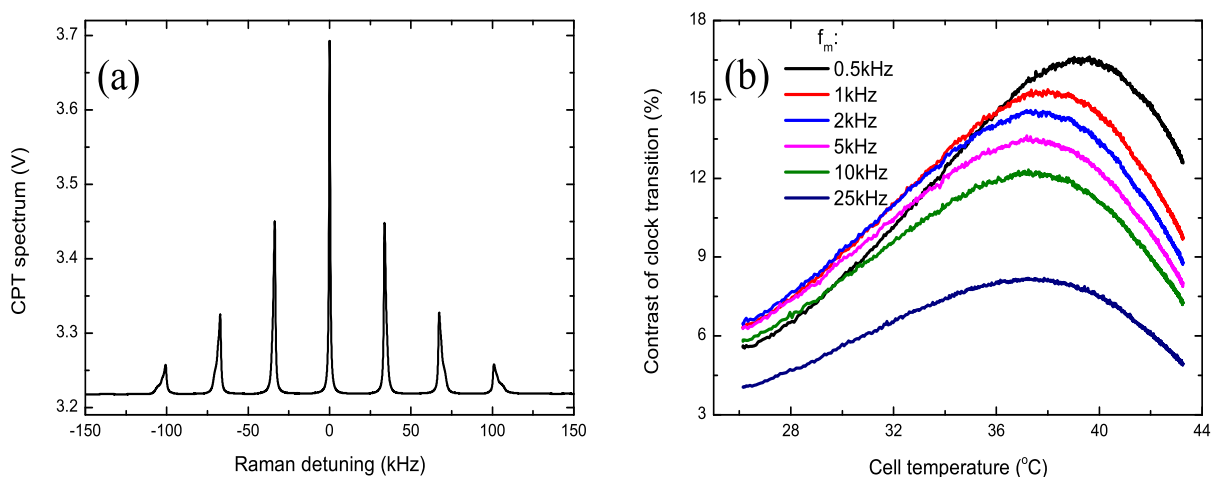


Figure 2: (a) Zeeman CPT spectrum obtained with a cw double-modulation with $f_m = 2$ kHz. (b) (Color online) CPT contrast vs cell temperature at various f_m . In both cases, $t_d = 3.5$ ms, $t_w = 0.5$ ms. Laser power: 1 mW.

The contrast of the clock transition, defined as CPT amplitude divided by the background level, reaches its maximum at the cell temperature of 37.5 °C in the case of $f_m = 2$ kHz as shown in figure 2(b). The optimal temperature shifts to a lower value as f_m increased.

We study the effect of modulation frequency f_m on the clock contrast at different detection window times as presented in figure 3(a). The highest CPT contrast is obtained around 1 kHz with a broad range of modulation frequency. This releases the requirements on the polarization switch, thus it is possible to further reduce the size of our laser system by utilizing a liquid crystal

polarization switch. When f_m is in the range from 500 Hz to 20 kHz, the contrast increases for short detection windows t_w . It begins to saturate at longer detection delay time t_d as illustrated in figure 3(b).

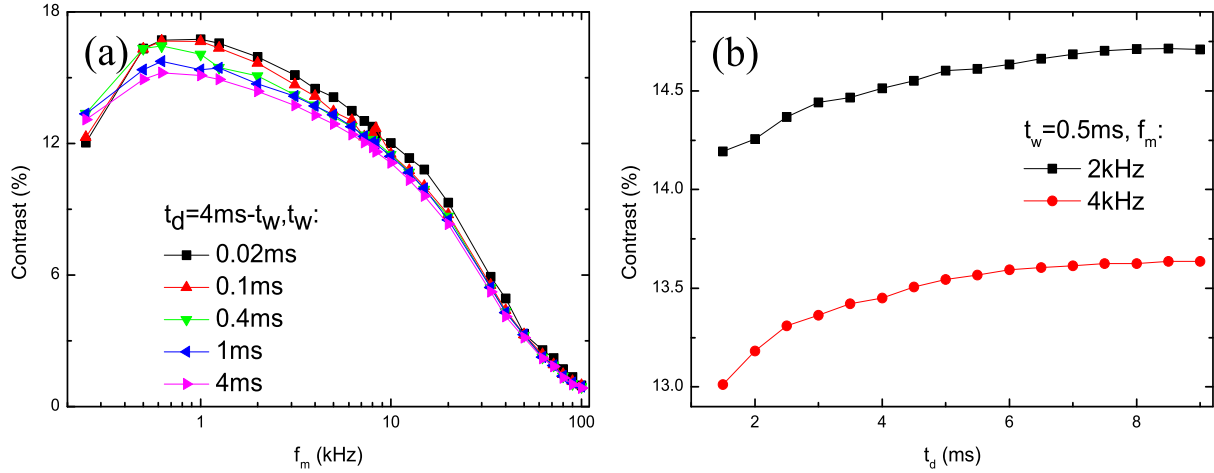


Figure 3: (Color online) (a) Contrast of clock transition as function of polarization modulation frequency f_m for several detection window durations t_w , $t_d = 4 \text{ ms} - t_w$. (b) Contrast vs t_d at two f_m values (2 and 4 kHz). In both cases, Laser power: 1 mW.

3.2. Clock signal and laser noise

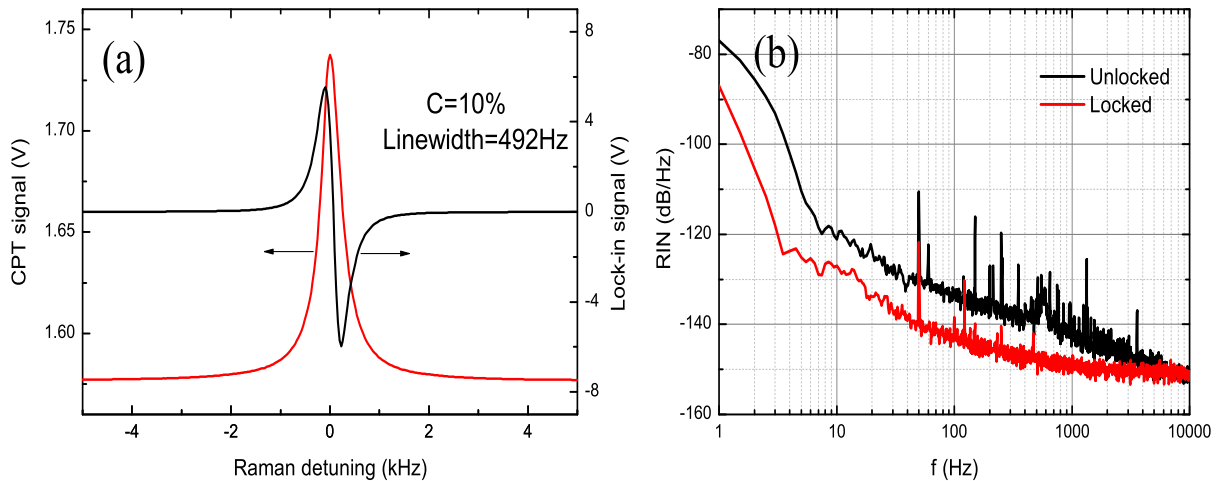


Figure 4: (Color online) (a) CPT signal and lock-in output signal of clock transition with $f_m = 2 \text{ kHz}$, $t_d = 3.5 \text{ ms}$, $t_w = 0.5 \text{ ms}$, $FM = 125 \text{ Hz}$, $\Delta_{FM} = 320 \text{ Hz}$. Laser power: 0.5 mW. (b) Relative intensity noise of our laser beam with and without power locking.

The signal of the clock transition, recorded with a laser power of 500 μW , is demonstrated in figure 4(a). The linewidth is 492 Hz and the contrast 10%. The error signal (figure 4(a)) is obtained after demodulation of the clock signal, square-wave frequency modulated as described in figure 1(b). The chosen modulation frequency, 125 Hz, is a compromise between a fast modulation reducing the noise level, and the time needed to accumulate the atomic population in the clock states.

As the laser relative intensity noise (RIN) usually is the main limitation to the short term frequency stability of CPT clock [6, 7, 11], a laser power locking set-up is employed. It utilizes an acousto-optic modulator, not drawn in figure 1(a), positioned between the EOPM and the polarization modulator. The RIN of the laser beam measured after the EOPM with and without power locking are displayed in figure 4(b). In the locked laser power case, the measured RIN is -142 dB/Hz at 125 Hz. With the CPT signal obtain in figure 4(a) and if this RIN level could be maintained after travelling through the atomic cell, the RIN limited frequency stability would be at level of 4×10^{-14} at 1 second. However, the light-atom interaction in the vapor cell is known to add tens of dB to the intensity noise. This point is now under investigation.

4. Conclusion

To implement a high performance CPT clock based on double-modulation method, we have investigated the optimal cell temperature and polarization and phase modulation frequency in cw mode. The optimal modulation frequency around several kHz implies we can utilize a liquid crystal polarization switch to further reduce the size of our clock. The duration and delay of the detection window are also addressed. The observed high contrast (10%) and narrow linewidth (492) Hz clock signal should lead to a frequency stability of 4×10^{-13} at 1 second if the laser RIN can be kept below -122 dB/Hz after crossing the vapor cell.

Acknowledgments

We would like to thank David Holleville, Thomas Zanon-Willette, Natascia Castagna, Jean-Marie Danet, Olga Kozlova, Stephane Trémine and Luca Lorini for helpful discussions. We are grateful to José Pinto Fernandes, Michel Lours and Electronic service at SYRTE for technical assistance and the realization of various electronic devices, Pierre Bonnay and Annie Gérard for manufacturing Cs cells. We thank Candy Xiong for reading of the manuscript. P. Y. is supported by the Facilities for Innovation, Research, Services, Training in Time & Frequency (FIRSTTF). This work is supported in part by ANR and DGA (ISIMAC project ANR-11-ASTR-0004). This work has been funded by the EMRP program (IND55 Mclocks). The EMRP is jointly funded by the EMRP participating countries within EURAMET and the European Union.

References

- [1] Camparo J 2007 *Physics Today* **60** 33
- [2] Godone A, Levi F, Calosso C E, Micalizio S 2015 *Riv. Nuovo Cimento* **38** 133-171
- [3] Bandi T, Affolderbach C, Stefanucci C, Merli, Skrivervik A K And Mileti G 2014 *IEEE Trans. Ultrason. Ferroelectr. Freq. Cont.* **61** 1769
- [4] Micalizio S, Calosso C E, Godone A and Levi F 2012 *Metrologia* **49** 425-436
- [5] Kang S, Gharavipour M, Affolderbach C, Gruet F and Mileti G 2015 *J. Appl. Phys.* **117** 104510
- [6] Danet J M, Kozlova O, Yun P, Guérandel S and de Clercq E 2014 *EPJ Web of Conferences* **77** 00017
- [7] Abdel Hafiz M and Boudot R 2015 *J. Appl. Phys.* **118** 124903
- [8] Alzetta G, Gozzini A, Moi L and Orriols G 1976 *Nuovo Cimento B* **61** 5
- [9] Vanier J 2005 *Appl. Phys. B* **81** 421
- [10] Zanon T, Guérandel S, de Clercq E, Holleville D, Dimarcq N and Clairon A 2005 *Phys. Rev. Lett.* **94** 193002
- [11] Danet J M, Lours M, Guérandel S and de Clercq E 2014 *IEEE Trans. Ultrason. Ferroelectr. Freq. Cont.* **61** 567
- [12] Jau Y Y, Miron E, Post A B, Kuzma N N and Happer W 2004 *Phys. Rev. Lett.* **93** 160802
- [13] Liu X C, Mérola J M, Guérandel S, Gorecki C, de Clercq E and Boudot R 2013 *Phys. Rev. A* **87** 013416
- [14] Yun P, Danet J M, Holleville D, de Clercq E and Guérandel S 2014 *Appl. Phys. Lett.* **105** 231106
- [15] Huang M and Camparo J C 2012 *Phys. Rev. A* **85** 012509
- [16] Yun P, Mejri S, Tricot F, Holleville D, de Clercq E and Guérandel S 2015 *Proc. Joint Conf. IEEE Int. Frequency Control Symp. - European Time and Frequency Forum IFCS-EFTF* (April 12-16 Denver, USA) p 797
- [17] Kozlova O, Danet J M, Guérandel S, and de Clercq E 2014 *IEEE Trans. Instrum. Meas.* **63** 1863